

## Central Lancashire Online Knowledge (CLOK)

Title	Can whole building energy models outperform numerical models, when forecasting performance of indirect evaporative cooling systems?
Type	Article
URL	<a href="https://clock.uclan.ac.uk/id/eprint/38809/">https://clock.uclan.ac.uk/id/eprint/38809/</a>
DOI	<a href="https://doi.org/10.1016/j.enconman.2020.112886">https://doi.org/10.1016/j.enconman.2020.112886</a>
Date	2020
Citation	Badiei, Ali, Golizadeh Akhlaghi, Yousef, Zhao, Xudong, Li, Jing, Yi, Fan and Zhanguyan, Wang (2020) Can whole building energy models outperform numerical models, when forecasting performance of indirect evaporative cooling systems? Energy Conversion and Management, 213 (112886). ISSN 0196-8904
Creators	Badiei, Ali, Golizadeh Akhlaghi, Yousef, Zhao, Xudong, Li, Jing, Yi, Fan and Zhanguyan, Wang

It is advisable to refer to the publisher's version if you intend to cite from the work.  
<https://doi.org/10.1016/j.enconman.2020.112886>

For information about Research at UCLan please go to <http://www.uclan.ac.uk/research/>

All outputs in CLOK are protected by Intellectual Property Rights law, including Copyright law. Copyright, IPR and Moral Rights for the works on this site are retained by the individual authors and/or other copyright owners. Terms and conditions for use of this material are defined in the <http://clock.uclan.ac.uk/policies/>

# Can Whole Building Energy Models Outperform Numerical Models, When Forecasting Performance of Indirect Evaporative Cooling Systems?

A. Badiei<sup>1,\*</sup>, Y. G. Akhlaghi<sup>1</sup>, X. Zhao<sup>1</sup>, J. Li<sup>1</sup>, F. Yi<sup>1</sup>, Z. Wang<sup>1,2</sup>

<sup>1</sup>Research Centre for Sustainable Energy Technologies, Energy and Environment Institute,  
University of Hull, Hull, HU6 7RX, UK

<sup>2</sup>School of Civil and Transportation Engineering, Guangdong University of Technology,  
Guangzhou, P.R. China, 510006

\*Corresponding author: [A.Badiei@Hull.ac.uk](mailto:A.Badiei@Hull.ac.uk); Tel.: +44 (0) 1482 86 3611

## Abstract

This paper presents a whole building energy modelling work incorporating a state-of-the-art indirect evaporative cooling system. The model is calibrated and validated with real-life empirical data, and is capable of representing actual performance of the system with high reliability. The investigated system is a novel super-performance Dew Point Cooler (DPC) with a guideless and corrugated Heat and Mass Exchanger (HMX). The DPC is modelled as part of the whole building energy model through detailed description of system and building characteristics at source code level. The developed model has been simulated in all different climates that an Indirect Evaporative Cooling (IEC) system can be operated, namely: subtropical hot desert, humid continental, Mediterranean, and hot desert climates. The performance predictions has been tested against experiments and numerical model of the same system, and a detailed investigation of modelling approaches to efficiently and effectively model aforementioned systems has been provided.

The calibrated and empirically validated whole building energy model predicted the key performance parameters of the dew point evaporative cooling system with mean error values limited to 4.1%. The highest COP values recorded by experiments and whole building energy simulations were 51.1 and 49, respectively. The whole building energy model proved to better predict the performance of dew point evaporative cooler, when compared to numerical models, by incorporating the building-side parameters into the model. This modelling work paves the way toward detailed investigation of the advanced cooling systems within building context to achieve optimised performance of the system in wide range of buildings and operating conditions.

**Keywords:** *Dew Point Cooler; Building energy; Model; Performance; Experiment*

## 1. Introduction

### 1.1. Background

The rapid growth in global energy consumption, especially in past decades, has raised the world-wide concern over security of supply as the existing energy resources are exhausting [1]. One of the main contributors to the rising global energy consumption is the service sector which covers all the commercial and public buildings with a wide range of HVAC system [2]. The global energy consumption of service sector has increased by 295 Mtoe in 2018 compared to 2000 levels and with this trend the sector would consume a further 323 Mtoe by 2040. The sector has also showed the least reduction potential in energy consumption under the Sustainable Development Scenario, compared to Industry, Residential and Transport sectors [1]. To deal with the high energy consumption levels associated with the service sector and to improve its poor performance under future scenarios, the focus has been shifted toward development of advanced, efficient and low-energy HVAC solutions in recent years.

The growing energy use by HVAC systems are particularly significant in developed countries. In the USA, HVAC energy use accounts for up to 50% of building energy consumption [3] while in china the HVAC energy use is between 50-70% of the total energy consumed in buildings [4]. Issac and Vuuren [5] estimated that energy demand associated with air-conditioning will rise rapidly in 21<sup>st</sup> century reaching a peak of 4000 TWh in 2050 and more than 10,000 TWh by 2100. There are other studies which have predicted a similar rise in energy demand of air-conditioning [6] under future weather conditions of USA [7], Switzerland [8], and Australia [9].

### 1.2. Air-conditioning: past, present and future

Traditionally, the most dominant air-conditioning systems were Mechanical Vapour Compression (MVC) ones which due to their inefficient compressors consumed a considerable amount of electricity [10]. In past decades absorption and adsorption cooling systems have gained more interest over mechanical vapour compression systems due to their lower energy consumption. The absorption and adsorption cooling systems greatly owe their lower energy consumption to replacing energy-intensive compressor with a cycle of high temperature water or vapour which reduces the applicability of these systems in sites with no access to heat source. Complexity of the pressurised and de-pressurised units used in the absorption and adsorption cooling systems and high maintenance costs associated

with them are other shortcomings of these systems which have raised the need for practical solutions [11].

The most recent approach to provide conditioned air is based on the fundamentals of evaporative cooling which relies on latent heat of water (both recyclable and renewable) to remove dissipated heat from conditioned spaces. The Dew Point Evaporative Cooling approach was first investigated by Dr Valeriy Maisotsenko [12] and the resultant technology is adeptly known as M-cycle cooling [3]. Evaporative cooling systems generally fall under two categories: Direct Evaporative Cooling (DEC) and Indirect Evaporative Cooling (IEC) based on whether the primary air is in direct contact with cooling water or not. In DEC, the direct contact between primary air and cooling water results in production of cooled but more humid air which provides reduced occupant comfort and is not suitable for high-tech facilities like data centres. IECs, on the other hand, separate the primary air and the cooling water by introducing dry and wet channels which cools the product air through the heat transfer between the two channels [13]–[15]. While IECs provide better indoor air quality compared to DEC, they have a lower heat removal capacity due to the constraints introduced by air's wet-bulb temperature.

To overcome the shortcomings of IECs, Dew Point Coolers (DPC) as the most advanced indirect evaporative cooling systems available in the market, offer a modified heat and mass exchanger (HMX) configuration to provide pre-cooling for the air in wet channels, eliminate the wet-bulb limits, and lower the product air temperature down to its dew point, thus improving the cooling efficiency by up to 30% compared to conventional IECs [3], [16]–[19].

### *1.3. Dew Point Coolers*

The research on Dew Point Coolers (DPCs) has gained more interest in past decade with first published work dating back to 2006 by Coolerado® project in USA [16] where a cross-flow HMX DPC with perforated holes on the flow path was tested. Results indicated that by employing this type of HMX, for the first time, wet-bulb and dew-point effectiveness of up to 80% and 50%, respectively could be achieved under specific operational conditions [16]. Since the first successful investigation and implementation of DPCs, more research has considered the potentials of these advanced cooling systems and recorded wet-bulb and dew-point effectiveness has reached values as high as 114% and 84%, respectively by Riangvilaikul et al. [20]. In their study a novel, vertically positioned DPC with counter-flow configuration between the intake and working air, and between the working air and water was tested experimentally.

Other example of experimental works on DPCs is a flat-plate cross-flow HMX DPC by Bruno [21] that used a special sheet with high water retention and wicking capability as the wet material layer, and a water-proof membrane as a dry material layer. The authors reported they were able to achieve an average dew-point effectiveness of 75%, which was relatively higher than that of the existing types for the same operational conditions. Xu et al. [4] performed an experimental analysis of a DPC prototype employing a super performance wet material, intermittent water supply configuration and a corrugated HMX to find wet-bulb and dew-point effectiveness of up to 114% and 75%, respectively, and a record-high COP of 52.5. The performance of same prototype DPC was then examined by Akhlaghi et al. [22] under four different climatic conditions, namely humid continental, Mediterranean, sub-tropical hot desert, and hot desert climates. Annual energy savings of up to 90% was achieved compared to the conventional MVCs.

With increasing demand for even more efficient and low-energy DPCs various modelling techniques and simulation tools have been employed by researchers across the world to investigate complex HMX configurations, water supply patterns, dry and wet channel materials, varying operating conditions and space requirements [20]–[36]. The modelling research on DPCs is investigated critically in the next section with particular attention to experimental validation of model outputs and observed uncertainties, advantages and limitation various modelling approaches introduce, and how this study fills the existing research gap on DPC research topic.

#### *1.4. Modelling DPCs: advantages, limits and the gap*

The vast majority of research on DPCs has employed numerical modelling techniques. Hasan [30] employed an analytical model of a regenerative indirect evaporative cooling trying to achieve sub-wet bulb temperature without the need for a vapour compressor. The results of analytical model was compared with a previously developed numerical model and some tests, and the recorded agreement of results ensured validity of system performance modelling [30]. Cui et al. also developed a numerical model of a evaporative dew point cooler [32] and investigated the performance of system under three improved scenarios namely, varying channel dimensions; employing room return air as the working fluid; and installation of physical ribs along the channel length [37]. Their model was validated through comparison of temperature distribution and outlet air conditions with experimental results, and the largest discrepancy was recorded as  $\pm 7.5\%$ .

Lin et al. [33] employed a transient and dynamic numerical model to take into account the dynamic transitions between various components of a DPC and validated the model through

inter-model comparison with a steady-state model of the same DPC and experimental comparison which yielded 4.3% discrepancy. Pandelidis et al. performed two numerical studies, one to investigate heat and mass transfer processes in an M-cycle HMX of a DPC [34] and the other to optimize the performance of the same evaporative air cooler [35]. In both studies experimental data was used to ensure the validity of model results and the optimal range of operational and geometrical conditions were identified. Akhlaghi et al. [38] developed a statistical model of a novel DPC employing Multiple Polynomial Regression (MPR) technique to predict the performance of the system. Several operating parameters including intake air temperature, relative humidity and flow rate as well as overall cooling capacity, Coefficient of Performance (COP), and wet bulb efficiency were investigated before applying the model to a number of scenarios in dry climates.

Sohani et al. [36] used a Neural Network (NN) based numerical model to study and optimise the performance of a DPC with M-cycle under 12 diverse climatic weather conditions. While the multi-objective optimisation technique used by authors was able to improve mean values of the COP and cooling capacity by 8.1% and 6.9%, adequate evidence on empirical validation of the model was not provided. Chen et al. [24] employed a experimentally validated numerical model of an IEC to perform a detailed sensitivity analysis and optimisation based on the most influential and practically controllable parameters. Xu et al. [28] also did a numerical modelling work on guideless irregular HMX with corrugated heat transfer surface as used in a novel DPC. The experimentally validated work proved that the novel DPC system was capable of achieving up to 37% more cooling capacity, 55.8% higher wet bulb efficiency, and 33.3% higher COP.

Other studies by Moshari and Heidarnejad [23], Akhlaghi et al. [39], [22], Rianguilaikul [20], [26], and Jradi et al. [27] all performed some sort of numerical modelling exercise in IECs and validated their findings through comparison with experimental data and other models. While all these studies were successful in recording some or extraordinary improvements in performance of the investigated systems, the vast majority of improvements were recorded under controlled test conditions in laboratory environment, neglecting the extensive building and occupants' interactions which happen in real world.

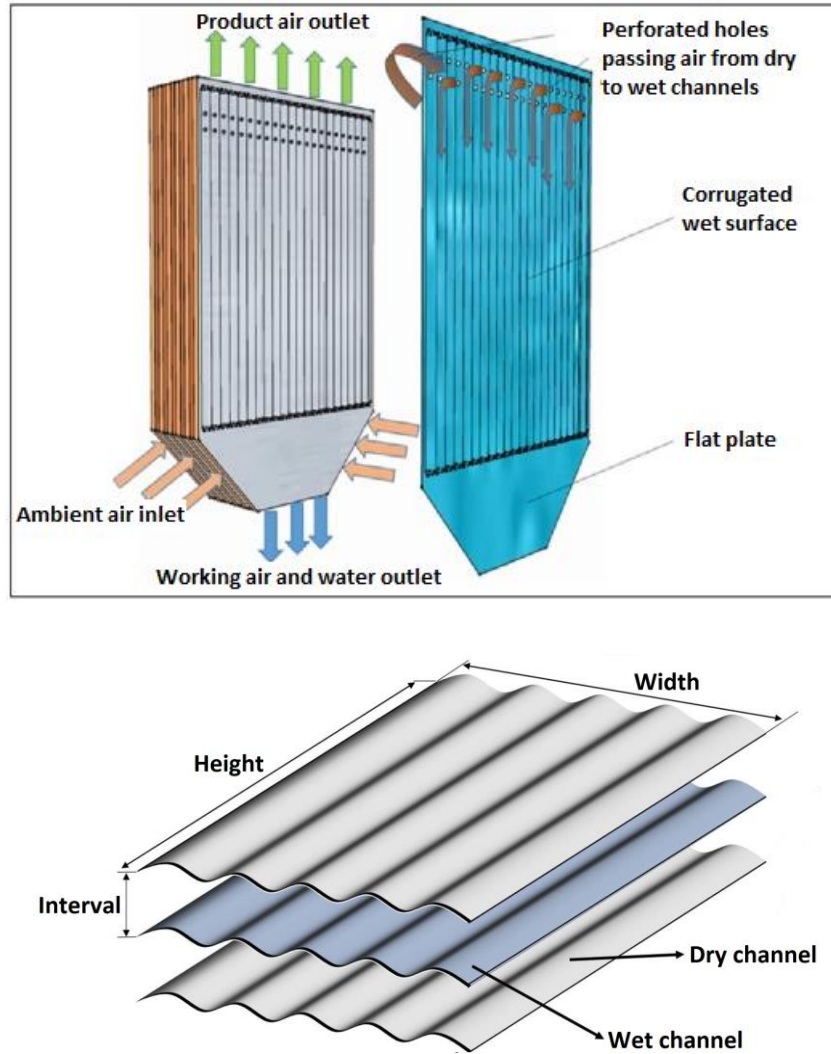
This study, therefore, fills the existing gap in DPC research by investigating the performance of a novel dew point evaporative cooling system through whole building energy modelling where the restraining system interactions with hosting building and its occupants are captured. In this way the transient behaviours of the system within the building envelope are quantified and the resultant impact on performance parameters of the system is investigated. A comparison of the predicted performance parameters from whole building energy

simulation to those from numerical models of the same system enabled the critical assessment of each modelling approach in dealing with advanced Indirect Evaporative Cooling (IEC) systems.

## 2. System Description

This study investigates a state-of-the-art, high-performance counter flow DPC employing a complex, 4 kW rated Heat and Mass Exchanger (HMX). The new HMX configuration replaces the channel support guides with a corrugated heat transfer surface separating dry and wet channels (as depicted in **Figure 1**) which decreases air flow resistance by up to 56% and increases heat transfer area by up to 40% leading to an improved heat transfer rate [28]. As seen in Figure 1 (a), a number of perforated holes are designed on top of each corrugated sheet to allow partial flow of air from dry channels to wet ones in order to complete heat transfer cycle and cool down the air in dry channels. The dry channels are made of a specific aluminium with high malleability while the wet channels' material is a flexible *Coolmax*<sup>®</sup> fibre with high water absorption, diffusion and evaporation capacities which allows the sheet to have corrugated shape. The geometric dimensions of the HMX is summarised in **Table 1**.

When system operates, the air with relatively high temperature and moisture level enters the DPC and passes through the dry channel losing its heat to the adjacent wet channel reducing its temperature to the desired level. Upon reaching the end of dry channel a part of cooled air leaves the channel as product air (to the conditioned space) and the remaining air is transferred to the wet channels through perforated holes as working air. This working air then gains heat from adjacent dry channel and moisture from *Coolmax*<sup>®</sup> material while passing through the wet channel and is discharged as exhaust air and water drops. In comparison to conventional flat plate HMXs, the introduced HMX configuration reduces the airflow resistance, increases heat transfer area, has higher diffusion area and better evaporation owing to use of *Coolmax*<sup>®</sup> wet channel material.



192 **Figure 1** Heat and Mass Exchanger (HMX). Upper: configuration and structure, Lower:  
 193 corrugated heat transfer surfaces separating dry and wet channels [38]

194 Owing to the high absorption capacity of fibrous material in the wet channels, the intermittent  
 195 water supply scheme was used by a dedicated water distributor system, which reduces the  
 196 amount of water used as well as water pump power consumption. The water distributor is  
 197 composed of a water pump, a water header, a water sink, and a water distributor tubes  
 198 which enable the even distribution of water over the surface of wet channels. When the  
 199 water sink underneath the HMX is empty, the water is supplied with flow rate of 6.85 L/min  
 200 for 15 seconds with 10 minutes intervals, and when the tank is full, the water is supplied with  
 201 flow rate of 2.45 L/min for 60 seconds with 10 minutes intervals.

202 In addition to the complex HMX introduced above, the DPC also employs two supply and  
 203 two exhaust air fans each with 160 W power, 458 Pa pressure, and 705 m<sup>3</sup>/h volumetric flow  
 204 rate, one circulating water pump with 24V DC power and 450 L/h flow rate, and two



205 controllers for the fans and the water pump. **Table 2** summarises the key elements of the  
 206 DPC system and associated technical specifications.

207 **Table 1** Geometric dimensions of the Heat and Mass Exchanger

Inlet flat plate height	120	mm
Outlet flat plate height	10	mm
Corrugated plate height	860	mm
Transition length between flat and corrugated plates height	5*	mm
Number of corrugated plates	160	-
Total height of the HMX	1000	mm
Width	800	mm
Length	358	mm
Total heat transfer area	49.3	m <sup>2</sup>
Height of corrugated wave	2.8	mm
Width of corrugated wave	11.6	mm

\*on each of the inlet and outlet sides

208 **Table 2** Technical manufacturer specifications of the DPC components

Component	Specifications
Supply air fan	R3G225-RE07-03, ebm-papst Ltd, fan speed 2865 rpm, 705 m3 .h <sup>-1</sup> , 458 Pa, 160 W
Exhaust air fan	R3G225-RE07-03, ebm-papst Ltd, fan speed 2865 rpm, 705 m3 .h <sup>-1</sup> , 458 Pa, 160 W
Water pump	DH40H-24110, Shenzhen Zhongke Century Technology, 24 V/1.2 A DC, 11mH <sub>2</sub> O, 450 L/hr
Fan controller	980-CAS11007 – TMS Controller, ebm-papst Ltd
Pump controller	DH48S-S, Xinling Electrical Co. Ltd

209 **Figure 2** represents the whole system design, the computer model, and the actual system in  
 210 the laboratory environment.

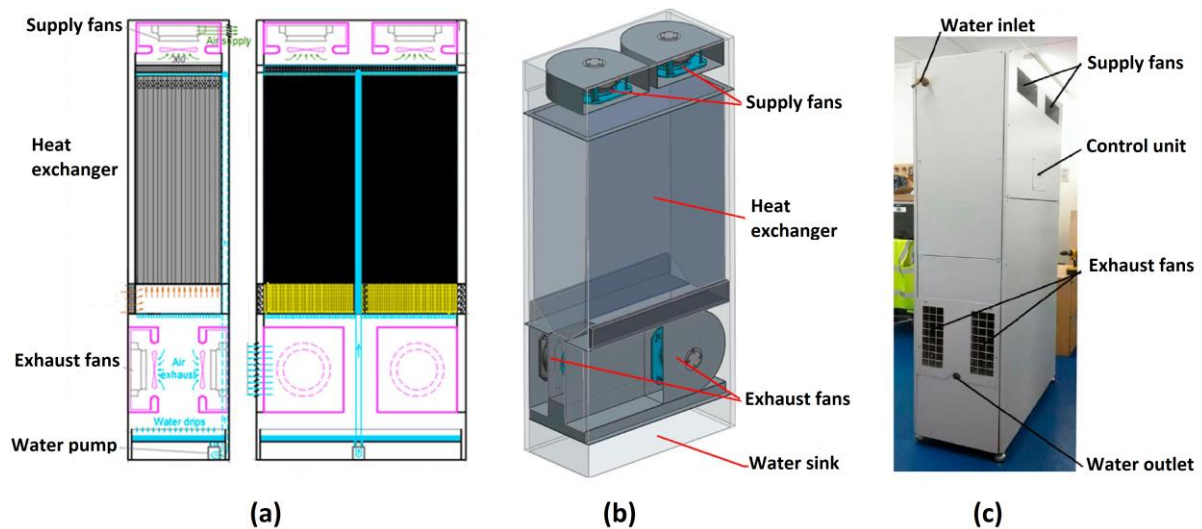


**Figure 2** Dew Point Cooler (DPC) and its components. (a): 2D cross-section view, (b) 3D computer model, (c): actual system in the lab environment [4]

Finally, for optimum operation of the DPC, temperature of the running water is kept at the range of 16-20°C to ensure efficient cooling [4]. A water filter with cartridge to purify the water and an anti-scale agent was used to minimise the risk of blockage at the perforated holes. Also an optimised water distribution scheme was introduced to maximise the use of circulating water within the cooler and reduce the amount of intake water [4].

### 3. Experimental Set-up and Analysis Method

To examine performance of the novel 4 kW Dew Point Cooler (DPC) with introduced complex Heat and Mass Exchanger (HMX), the test set-up presented in **Figure 3** was constructed in the lab environment. The test set-up comprises a heater, a humidifier/dehumidifier, and four balancing dampers to enable conditioning of the inlet air and simulate various weather conditions.

The water pump, supply and exhaust fans, and supply-discharge ducting system is also presented in **Figure 3**. After conditioning the inlet air temperature and humidity to match those of the climates under study, the supply fans and the necessary ducting is used to create a zero static pressure at the inlet of DPC. A specific multi-function measurement device capable of measuring the ventilation and air conditioning parameters as well as indoor air quality parameters (i.e. temperature, humidity, flow rate and speed) was used to identify the characteristics of the air flow at the inlet and outlet of the system. The measurement points were placed at a distance 10 times the diameter of the ducts ( $\phi 160$  mm) from inlet and outlet of the system to allow development of fully steady air flow for the sake of accuracy of measurements. Two water flow meters were also installed at the inlet

and outlet of wet channels to measure the amount of water used and consequent pressure drop. A water pressure of 1.8 mH<sub>2</sub>O was preserved throughout the system to ensure even distribution of the water across the wet surfaces (as suggested by *Coolmax*<sup>®</sup> wet channel material manufacturer). Finally, a simple fan controller was employed to achieve the optimum working air to intake air ratio of 0.37, and product air and waste air flow rates of 602 m<sup>3</sup>.h<sup>-1</sup> and 364 m<sup>3</sup>.h<sup>-1</sup>, respectively, throughout the experiments as identified by [20].

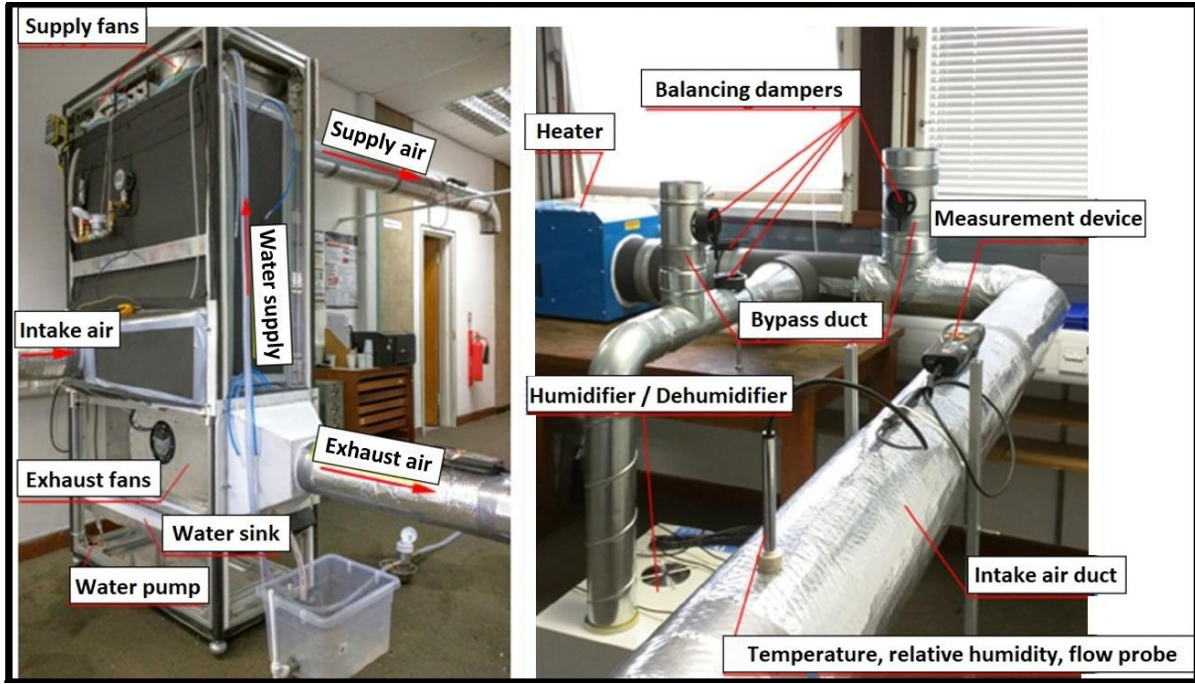


**Figure 3** Experimental test set-up with individual components as constructed in the laboratory environment

The measure parameters from the system are recorded in real time and analysed to quantify the overall cooling capacity, Coefficient of Performance (COP), wet bulb and dew point efficiencies. The overall cooling capacity of the system can be calculated from **Equation 1**, as suggested by ASHRAE [40] for all Indirect Evaporative Cooling (IEC) systems:

$$Q_{Cooling} = C_p(T_{dry,in} - T_{dry,out})(1 - \phi)Q_{m,dry,in} \quad \text{Equation 1}$$

Where  $Q_{Cooling}$  is the cooling capacity of DPC,  $C_p$  is the specific heat capacity of the inlet air,  $T_{dry,in}$  and  $T_{dry,out}$  are the inlet and outlet temperatures of the air in dry channel,  $\phi$  is the working air to intake air ratio, and  $Q_{m,dry,in}$  is the mass flowrate of the intake air in the dry channel.

252 Then the Coefficient of Performance (COP) can be calculated as the ratio of cooling capacity  
253 to the total of electrical power consumed by fans ( $W_{Fans}$ ) and pumps ( $W_{Pumps}$ ):

$$COP = \frac{Q_{Cooling}}{W_{Fans} + W_{Pumps}} \quad \text{Equation 2}$$

254 Finally, the wet bulb and dew point efficiencies ( $\varepsilon_{wb}$  and  $\varepsilon_{dp}$ ) are calculated from **Equation 3**  
255 and **Equation 4**, respectively:

$$\varepsilon_{wb} = \frac{T_{dry,in} - T_{dry,out}}{T_{dry,in} - T_{dry,in,wb}} \quad \text{Equation 3}$$

$$\varepsilon_{dp} = \frac{T_{dry,in} - T_{dry,out}}{T_{dry,in} - T_{dry,in,dp}} \quad \text{Equation 4}$$

256 Where  $T_{dry,in,wb}$  and  $T_{dry,in,dp}$  are the wet-bulb temperature of the intake air in dry channel  
257 and the dew point temperature of the intake air in dry channel, respectively.

258 Having identified the performance parameters needed to investigate the DPC, four  
259 representative cities with totally different weather conditions were identified to test the  
260 performance of system. These cities are: Las Vegas (USA) with subtropical hot desert  
261 climate, Beijing (China) with humid continental climate, Rome (Italy) with Mediterranean  
262 climate, and Riyadh (KSA) with hot desert climate. The weather conditions from these cities  
263 were simulated and corresponding intake air with representative temperature and humidity  
264 levels were produced in the laboratory environment to test the performance of DPC under  
265 each climate. Due to very high relative humidity of the air in Beijing and Rome, a pre-  
266 treatment had to been applied to the intake air in order to bring the humidity level to the  
267 operational range (<40%) of the DPCs in common high-tech facilities like data centres [39].  
268 Hence, this research could focus solely on the cooling performance of the system without  
269 having to take into account the dehumidification. The dehumidification process was carried  
270 out using a solar/waste energy driven dehumidification cycle employing a desiccant bed  
271 located inside a channel that is constructed by a porous and visible-light LiCl-Silicon-Gels  
272 material. As a result of the dehumidification process, the moisture content of outside air in  
273 Beijing and Rome are brought down required range resulting in a parallel sensible cooling  
274 process. The monthly average temperature and relative humidity of the four representative  
275 cities and corresponding pre-treated values for Beijing and Rome are all summarised in  
276 **Table 3**.

As seen in **Table 3** the temperature and humidity values are given only for the months where free cooling is not available in each particular climate and there is need for operation of DPC. The average outdoor temperature required for free cooling is identified as 22°C based on ASHRAE guidelines for power requirements in data centre design [41]. For Beijing and Rome weather conditions where pre-treatment was necessary, the pre-treated monthly temperatures are taken as the selection criteria. Hence, the DPC operation is required from March to October in Riyadh, from April to October in Beijing and Las Vegas, and from May to October in Rome as seen in **Table 3**.

**Table 3** Monthly average temperature and humidity values for the four representative cities with pre-treatment data where required

Month	Beijing				Rome				Las Vegas		Riyadh	
	Before pre-treatment		After pre-treatment		Before pre-treatment		After pre-treatment		No pre-treatment needed			
	T(°C)	RH	T(°C)	RH	T(°C)	RH	T(°C)	RH	T(°C)	RH	T(°C)	RH
March	-	-	-	-	-	-	-	-	-	-	27	37%
April	20	45%	23.7	16%	-	-	-	-	25	25%	31	35%
May	26	53%	30.8	23%	23	75%	27.3	39%	30	21%	38	21%
June	30	60%	35.6	24%	26	74%	30.8	35%	37	18%	42	16%
July	31	75%	36.8	24%	28	73%	33.2	38%	40	20%	44	17%
August	30	78%	35.6	40%	28	75%	33.2	39%	39	27%	42	19%
September	27	69%	32	35%	27	75%	32	39%	33	26%	42	19%
October	20	60%	23.7	28%	23	76%	27.3	40%	27	30%	35	23%

Having identified the intake air properties, the heater and humidifier/dehumidifier shown in **Figure 3** were used to produce the intended intake air for the DPC and then the DPC was operated under each weather conditions. The system performance parameters as well as the achieved indoor air properties were recorded and are presented in **Section 6**.

#### 4. Numerical Model of the System

A numerical model of the advanced Dew Point Cooler (DPC) with corrugated HMX design was developed using Multiple Polynomial Regression (MPR) technique [38]. Regression analysis is a very popular and well know method as it provides robust grounds for developing predictive tools to investigate complex relations between dependant and

independent parameters in a wide range of areas i.e. engineering, physics and chemical sciences [42], [43]. The developed model takes a set of operational and geometric parameters as input to predict the performance parameters of the DPC under investigation. These parameters and their corresponding ranges as used in the MPR model are summarised in **Table 4**.

**Table 4** Operational and geometrical parameters used in the MPR model to predict performance parameters of the DPC and the corresponding ranges

Operational Parameters	Range	Geometrical Parameters	Range	Performance Parameters
Intake air temperature, T(°C)	25-45	Channel height, H (m)	1-3	Cooling capacity
Intake air relative humidity, RH	0.125-0.5	Channel interval, Int (m)	0.004-0.008	Coefficient of Performance
Intake air flow rate, U (m/s)	0.3-3.3	Number of layers, L	100-200	Dew point effectiveness
Working air to intake air ratio ( $\varphi$ )	0.1-0.9	-	-	Wet-bulb effectiveness

The operating and geometrical parameters were used as independent parameters in the MPR model mainly due to the flexibility of these parameters which allows them to be changed continuously in real-life operation of the DPC. Hence, other parameters which didn't offer such flexibility were excluded from input parameters of the model.

**Table 5** Discrete values selected for operating parameters to construct training and validation sets of the MPR model [38]

No	Training set				Validation set			
	T (°C)	RH	U (m/s)	$\varphi$	T (°C)	RH	U (m/s)	$\varphi$
1	25	0.125	0.3	0.1	26.25	0.14	0.5	0.15
2	27.5	0.17	0.7	0.2	28.75	0.19	0.9	0.25
3	30	0.22	1.1	0.3	31.25	0.24	1.3	0.35
4	32.5	0.26	1.5	0.4	33.75	0.28	1.7	0.45
5	35	0.3	1.9	0.5	36.25	0.32	2.1	0.55
6	37.5	0.34	2.3	0.6	38.75	0.36	2.5	0.65
7	40	0.38	2.7	0.7	-	-	-	-
8	42.5	0.42	3	0.8	-	-	-	-
9	45	0.5	3.3	0.9	-	-	-	-

Having identified the input (operational and geometrical) parameters and their ranges, discrete values for each parameter were required to construct a training set to develop the model and a validation set to verify the developed model. Hence, 9 discrete values for the training set and 6 discrete values for the validation set were selected to develop the MPR model (**Table 5**).

As seen in **Table 5** the discrete values for the two sets were chosen such that the validation set values won't overlap with training set values, hence offering robust model validation grounds. As for geometrical parameters, discrete values of 1m, 2m, and 3m for height, 0.0004m and 0.008 for interval, 100 and 200 for number of layers were used in the model (see **Figure 1** for geometrical parameters). Water temperature was modelled as 16°C and water flow rate as 411 L/h to match the experimental values [4]. All the possible combinations with these discrete values were considered in the model to account for all the random operating conditions. Hence, the total number of operating conditions becomes 7857 in which 80% of them, 6561 ( $9^4$ ), are for training set and 20%, 1296 ( $6^4$ ), are for the validation set. Once the model is developed and validated, it can be used beyond the scope of the discrete values and ranges presented in **Table 4** and **Table 5**.

The regression model was developed from the described data sets in R software package can be represented in the following equation:

$$Y = \beta_0 + \beta_1 \times (T^{n_{1,1}} \times RH^{n_{2,1}} \times U^{n_{3,1}} \times \varphi^{n_{4,1}}) + \beta_2 \times (T^{n_{1,2}} \times RH^{n_{2,2}} \times U^{n_{3,2}} \times \varphi^{n_{4,2}}) + \dots + \beta_m \times (T^{n_{1,m}} \times RH^{n_{2,m}} \times U^{n_{3,m}} \times \varphi^{n_{4,m}}) \quad \text{Equation 5}$$

Where  $Y$  represents all the performance parameters to be predicted by model,  $T$  is temperature,  $RH$  is the relative humidity,  $U$  is air flow velocity of intake air, and  $\varphi$  is the working air to intake air ratio.  $\beta_0, \beta_1, \beta_2, \dots, \beta_m$  are regression coefficients to represent geometric characteristics;  $n_{1,m}$  represents the intake air temperature of the  $m^{\text{th}}$  coefficient,  $n_{2,m}$  represents intake air humidity of the  $m^{\text{th}}$  coefficient,  $n_{3,m}$  represents intake air flow velocity of the  $m^{\text{th}}$  coefficient, and  $n_{4,m}$  represents the working air to intake air ratio of the  $m^{\text{th}}$  coefficient.

The model was developed based on the introduced training sets and the validation set was used to verify the predicted performance parameters ( $Y$ ). For validation purpose, least squares method was used where the sum of squared residuals are minimised. The residual or Sum Square of Errors (SSE) is the difference between the actual values and the estimated regression values by MPR model (also denoted as  $r_i$ ):

$$SSE = \sum_{i=0}^N (\hat{Y}_i - Y_i)^2 = \sum_{i=0}^N r_i^2 \quad \text{Equation 6}$$

Where  $\hat{Y}$  represents the predicted value of individual performance parameters, Y is the actual value of the same parameter, and N is the number of predicted value. Having identified the SSE value, three of the main metrics to evaluate the performance of the model i.e. Mean Square Error (MSE), Maximum Relative Error (MRE), and coefficient of determination ( $R^2$ ) can be calculated:

$$MSE = \frac{SSE}{N} = \frac{\sum_{i=0}^N (\hat{Y}_i - Y_i)^2}{N} = \frac{\sum_{i=0}^N r_i^2}{N} \quad \text{Equation 7}$$

$$R^2 = 1 - \frac{SSE}{SST} = 1 - \frac{\sum_{i=0}^N (\hat{Y}_i - Y_i)^2}{\sum_{i=0}^N (\bar{Y}_i - Y_i)^2} \quad \text{Equation 8}$$

Where SST is sum square of total, and  $\bar{Y}$  is the mean of predicted values.

## 5. Whole Building Energy Model

The whole building dynamic energy model of the system and the hosting building was developed using EnergyPlus (e<sup>+</sup>) software package (version 8.9.0.1) [44], which is open source, widely used and verified. In order to enable empirical validation and comparison with numerical model, the same system parameters and numerical model inputs as described in **Sections 2, 3 and 4** were used in developing the whole building energy model. Where there was lacking data, further data collection was conducted to create a detailed energy model which is capable of representing reality with high reliability.

To facilitate the data input process, DesignBuilder [45] software version 6.1.2.009 was employed to create laboratory building's geometry (where DPC was operated and tested), construction materials, internal boundary conditions and a template of an Indirect Evaporative Cooler (IEC). DesignBuilder was used initially because it is a commercially available software package that offers detailed dynamic thermal simulations, employing the EnergyPlus simulation engine and provides a user friendly graphical user interface [45].

Having formed the basis for energy model of the DPC in Laboratory environment, the corresponding EnergyPlus Input Data File (IDF) was exported with .idf extension. The IDF was then modified using a text editor and the EnergyPlus IDF editor [46] to add exact DPC characteristics as described in **Sections 2 and 3 (Figure 4)**. The completed IDF with custom weather files created for the four cities investigated in the experiments (see **Table 3** for



details) were fed to the EnergyPlus and simulations were run. As seen in **Figure 4** the simulation results were then checked against experimental results and necessary modification were added to the EnergyPlus IDF in order to produce the validated and calibrated model of the DPC under investigation.

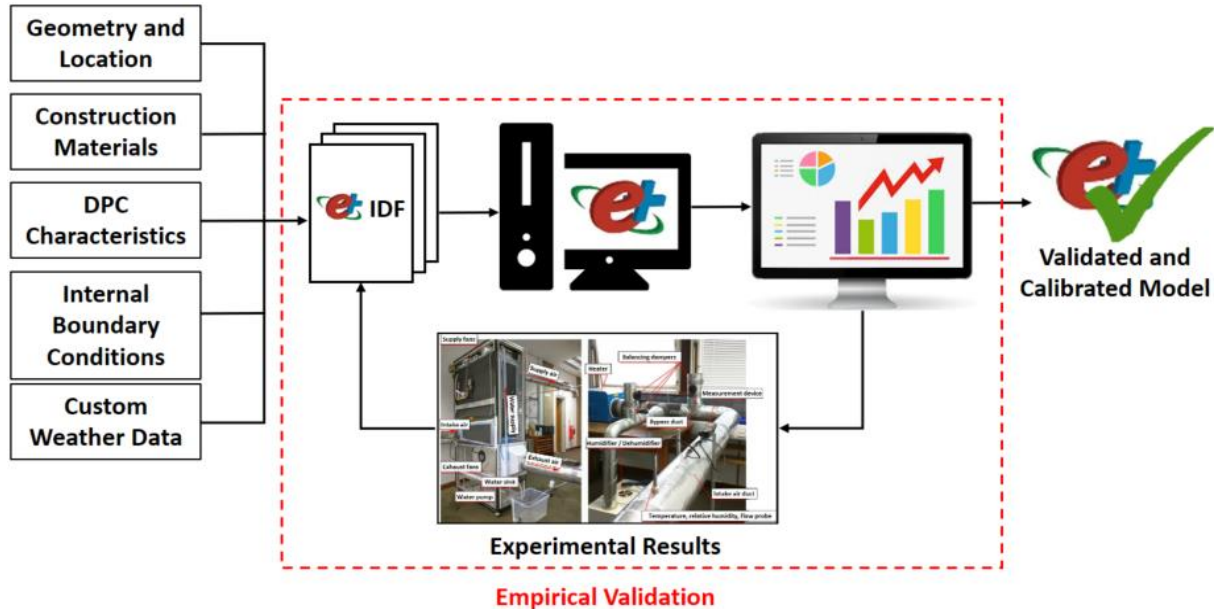


**Figure 4** Schematic of the whole building energy modelling process: from raw data to the validated model

Upon completion of the modelling process as depicted in **Figure 4**, the validated whole building energy model and the performance parameters predictions are compared to the numerical model estimates (**Section 6**).

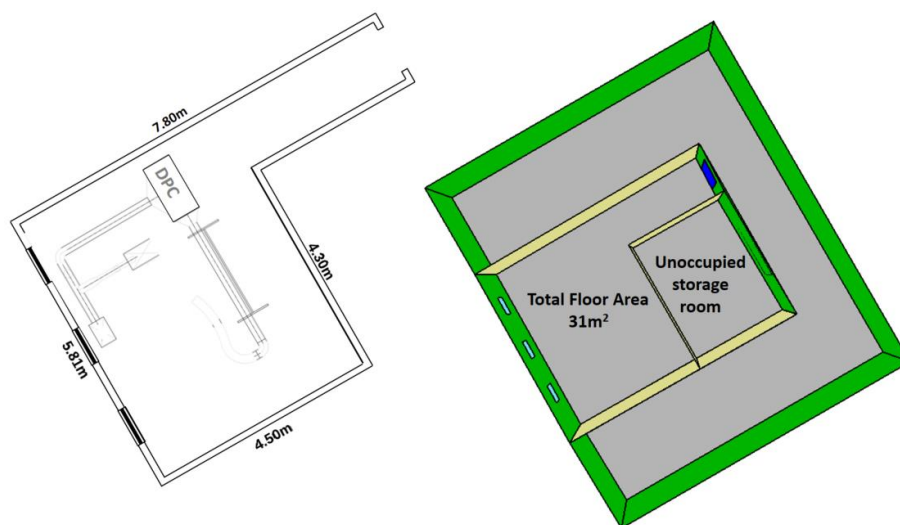


**Figure 5** Left: Floor plan of the laboratory room depicting DPC configuration, Right: Building layout with adjacent rooms to the laboratory as modelled in DesignBuilder

The building hosting the Dew Point Cooler (DPC) in experiments was modelled in EnergyPlus software package based on the data collected through a comprehensive survey carried out on the building. **Figure 5** presents the floor plan of the laboratory building with DPC test set-up, and a 2-D view of the building model.

As seen in **Figure 5** the adjacent spaces to the experiment room is also modelled in order to capture possible impact they can have on the indoor environment of the laboratory and consequently on system performance. The experiment room has total floor area of  $31\text{m}^2$  and floor to ceiling height of 2.7m with an L-shaped layout, three windows with total glazing area of  $1.1\text{m}^2$  and a wooden entrance door with area of  $1.6\text{m}^2$ . **Table 6** summarises the construction materials of the building, their compositions and their corresponding U-values as modelled in EnergyPlus. Since the construction details of the building wasn't a part of analysis in previous experimental or numerical modelling studies, the required details for developing the whole building energy model was gathered separately by surveying the building envelope and referring to building plans and construction handbook provided by states office at the University of Hull, where the DPC is tested. Hence, the description of construction materials and details of their layers were used in the modelling process and resultant U-values are reported in **Table 6**.

The external walls are made of lightweight concrete blocks as outermost layers followed by a thin air gap and plasterboard on the inside of the building, with an overall U-value of  $1.6\text{ W/m}^2\text{K}$ . The laboratory where the experiments were carried out was located on second floor of the building, hence the internal floor and ceiling was modelled as a solid concrete slab with U-value of  $0.7\text{ W/m}^2\text{K}$ . The room has three square windows, equally spaced on the external wall with single glazing and aluminium frame which were closed during the experiments and hence modelled with zero opening area and overall U-value of  $4.8\text{ W/m}^2\text{K}$ . The entrance door to the room was a wooden one with 65mm thickness and U-value of  $3.0\text{ W/m}^2\text{K}$ . Finally, the internal partitions separating the experiment room from the rest of building were formed of a single layer brickwork covered with plaster on each side giving the walls a thickness of 220mm and U-value of  $2.1\text{ W/m}^2\text{K}$ .

Measuring infiltration rates of the experiment room was not possible at the time of this study as the tests were running in the experiment room. Instead, airtightness test results of a similar laboratory in the same building which was carried out in 2017 and reported in building data repository was used. The airtightness test was carried out with 50 Pa pressurised unit and **Equation 9**, from BS EN 12831 [47] was used to convert the reported value to infiltration rate at normal operating conditions:

$$\dot{V}_{inf,i} = 2 \times V_i \times n_{50} \times e_i \times \varepsilon_i \quad \text{Equation 9}$$

Where  $\dot{V}_{inf,i}$  is the infiltration rate of the space,  $V_i$  is the volume of space ( $\text{m}^3$ ),  $n_{50}$  is the air exchange rate per hour (ACH), resulting from a pressure difference of 50 Pa between the inside and outside of the building,  $e_i$  is the shielding factor which was taken as 0.03 for a moderate shielding and heated spaces with more than one exposed opening, and  $\varepsilon_i$  is height correction factor which takes into account the increase in wind speed with the height of the space from ground level.  $\varepsilon_i = 1$  when the centre of zone height to ground level is below 10m which was the case in the experiment room. Inserting the infiltration value of 0.16 ACH (as result of airtightness test) into the **Equation 9**, an infiltration rate of 0.8 ACH was calculated and added to the whole building energy model of the building.

**Table 6** Summary of construction materials as modelled in EnergyPlus, physical properties, and corresponding overall U-values

Element	Description	Layers	Thickness (mm)	Density ( $\text{kg}/\text{m}^3$ )	Specific heat capacity ( $\text{J}/\text{kgK}$ )	U-value ( $\text{W}/\text{m}^2\text{K}$ )
External walls	Lightweight concrete block, air gap and plasterboard	Concrete block	200	600	1000	1.6
		Air gap	25	-	-	
		Steel	10	7800	450	
		Plasterboard	10	900	1000	
Internal floor/ceiling	Solid (concrete slab)	Cast concrete	150	2100	840	0.7
Windows	Single glazing with aluminium frame	Glazing	3	-	-	4.8
		Frame	35	2800	880	
Entrance door	Wooden	Painted oak	65	700	2390	3.0
Internal partitions	Solid Brick	Brick (inner)	220	1700	1000	2.1

The building was modelled as two thermals zones: the experiment room and the rest of the building. The heat gains from the system equipment were excluded from the zone definition as these details are included in the system model and the resultant impact on system performance and indoor environment is considered. The occupancy and the metabolic gains are also modelled to represent presence of a single person (to run the experiments) in the room during system operations and no window or door opening is considered to eliminate the impact of external air flow on system performance. Lighting gains of  $10 \text{ W}/\text{m}^2$  are also considered in the model.

The custom EnergyPlus weather files were created by scaling typical weather year data from the International Weather for Energy Calculations (IWECC) [48] following the methodology described in a previous article by the authors [49]. Monthly values of external air temperature and relative humidity were compared with the experimental weather values to produce a scaling factor. The scaling factor was then applied to the hourly values using EnergyPlus auxiliary weather programme [46] to produce equivalent weather information suitable for whole building energy modelling. For weather information from Beijing and Rome, the pre-treated values given in **Table 3** were used to develop the equivalent hourly weather file, whereas for Riyadh and Las Vegas the original values were used as no pre-treatment was found necessary.

The DPC was modelled explicitly in EnergyPlus by detailed modification of the IDF files including geometry and construction details. The dimension and size details of the system, as presented in **Figure 6**, were added into IDF files as object-oriented entries which sat in the previously allocated lines of the IDF as assigned by the system template.

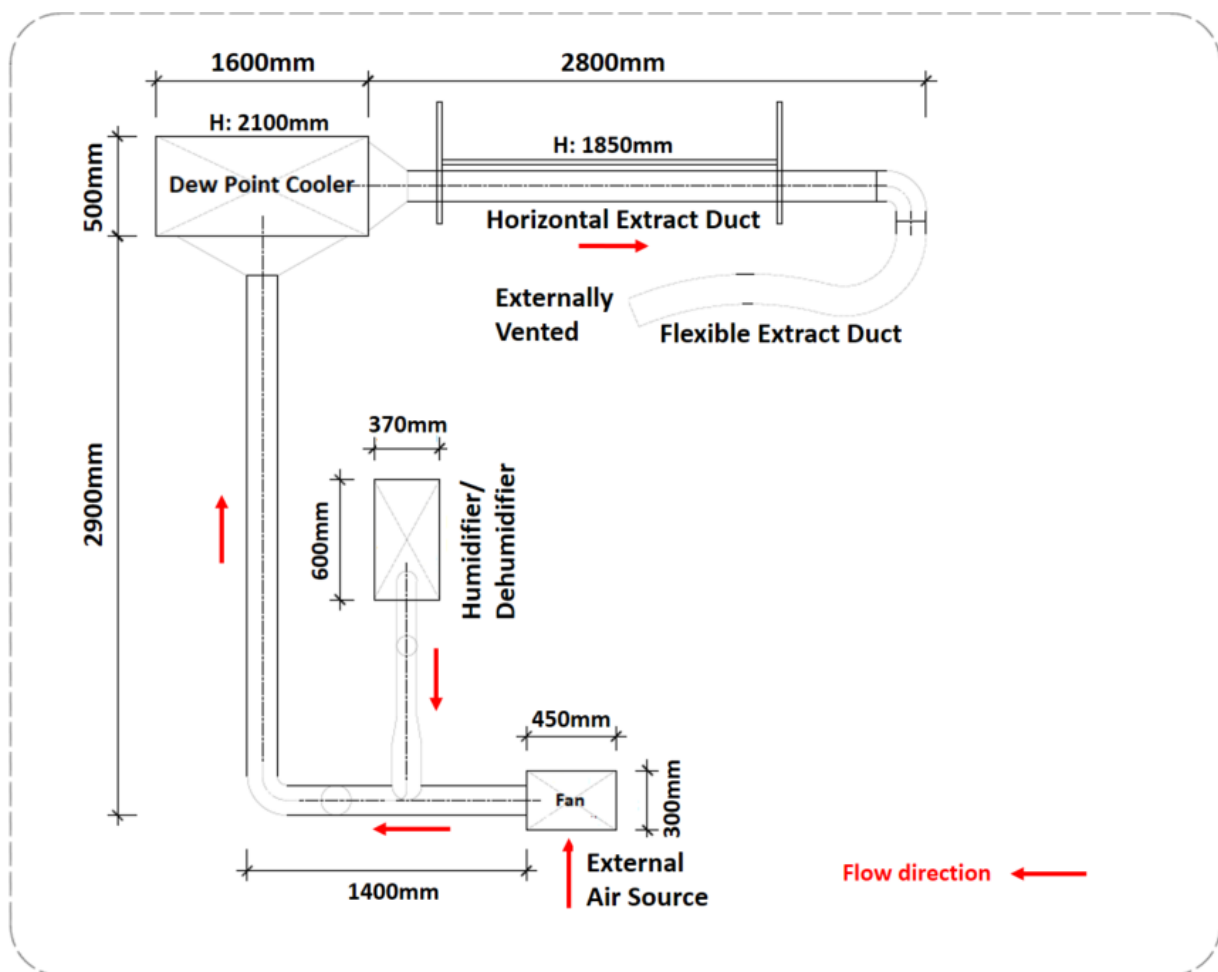


**Figure 6** Dew Point Cooler (DPC) and test set-up technical plan as constructed in laboratory environment with component dimensions

The overall power requirements of the pumps and fans (90.5 W), pressure rise range and efficiencies as identified in product catalogues, air flow rates passing through the wet and dry channels of the DPC as measured in the experiments (602 and 364 m<sup>3</sup>.h<sup>-1</sup>), and height of air inlets (2.1m) and outlets (1.85m) as depicted in **Figure 6** were all included the IDF's to ensure system model is capable of simulating real-life operation of the DPC.

The details of the system as constructed in the laboratory environment was input explicitly into IDF's except for the Thermal Mass Parameter (TMP). This was due to EnergyPlus not having the capacity to model system physically, instead the operation and performance of the system was modelled. Hence, the experiment room was modelled as a vacant space with conditioned air inlet and exhaust air outlets. To account for the TMP of system component, a further TMP of 50 kJ/m<sup>2</sup>K was added to the existing TMP of the building as calculated from **Equation 10** [50]:

$$TMP = \frac{\sum \kappa \times A}{TFA} \quad \text{Equation 10}$$

Where  $\kappa$  is the heat capacity (kJ/m<sup>2</sup>K) of each element,  $A$  is the element's area, and  $TFA$  is the Total Floor Area of the experiment room, and the summation is over all walls together with both sides of all internal walls and floors/ceilings.

## 6. Results and Discussion

### 6.1. Comparison of the whole building energy model results with experiments: empirical validation

The completed IDF's which were developed to represent the actual system and hosting building's characteristics under equivalent experimental conditions were fed to the EnergyPlus calculation engine and simulations were run for the previously identified climates (see **Table 3** for climate details). The model was calibrated and simulations were compared to experimental results in order to validate the model. All the simulations were run in EnergyPlus version 8.9.0.1, and simulation of system operation under each climate required approximately 18 minutes of single CPU time for a full year simulation at 1-minute time steps. The model was calibrated using the operational parameters contributing to cooling capacity of the system, as provided in **Equation 1**. The specific heat capacity of the inlet air ( $C_p$ ), the inlet and outlet temperatures of the air in dry channel ( $T_{dry,in}$  and  $T_{dry,out}$ ), and the working air to intake air ratio ( $\phi$ ) as modelled in EnergyPlus were checked against experimental values to ensure system model characteristics matched those of the actual system. Having calibrated the system model, simulation results were exported and analysed.

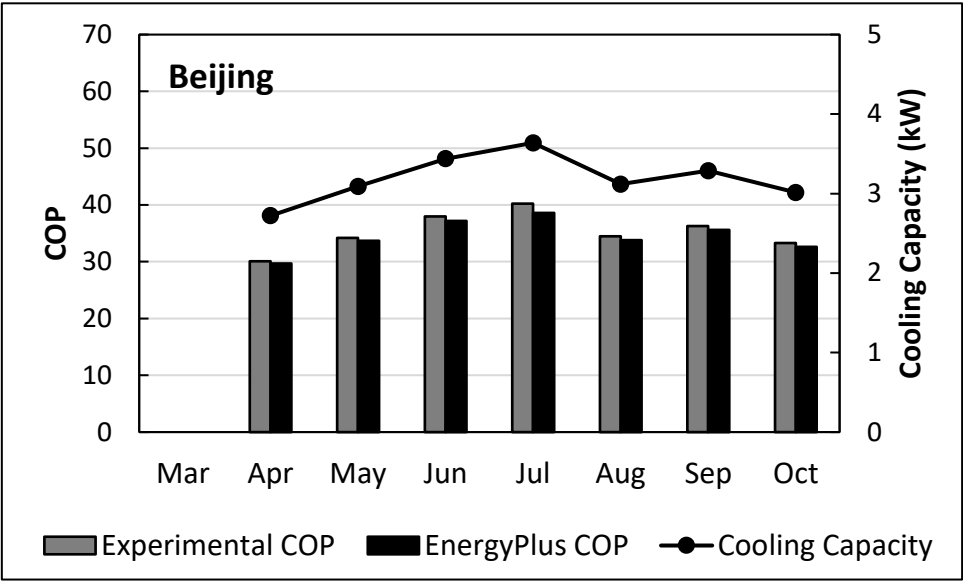
Figure 7 presents the comparison of experimental COP and cooling capacity results to EnergyPlus predictions in: (a) Beijing, (b) Rome, (c) Las Vegas, and (d) Riyadh. As seen in Figure 7, the cooling capacity of the actual system and simulations are identical to each other in all the simulated climates. This shows that the calibration of model using the mentioned operational parameters were reflected in the simulation results and the system model is capable of representing actual operation of the DPC. However, other performance parameters (as listed in **Table 4**) need to be checked to ensure that the whole building energy model is also accurate and capable of representing transient interaction of the system with surrounding building.

An initial look at the graphs in **Figure 7** reveals that both experimental and simulation values of the COP in all four of the climates follow a similar trend to cooling capacity variations throughout the year. The highest cooling capacity of the system and thus the highest power consumption was observed under hot desert weather conditions of the Riyadh and subtropical hot desert weather conditions of Las Vegas with cooling capacity reaching a peak of 4.6 kW in July.

The DPC was required to run for 180 minutes under each weather condition to allow system enough time to stabilize, and the rate of power consumption in Beijing, Rome, Las Vegas, and Riyadh as recorded by experiments were 12.77 kW, 10.21 kW, 13.56 kW, and 15.33 kW, respectively. In this study, the rate of power consumption by DPC under different weather conditions is considered instead of the amount of used electricity as the comparison factor. This is mainly because of different running times of the DPC in various regions and hosting facilities which are highly dependent on the weather conditions and the amount of dissipated heat as well as various operating time of facilities. Hence, the rate of power consumption was chosen as comparison factor in order to eliminate impact of inequivalent operating parameters on system performance. Considering the 24-hour operation of DPC during the operating months (as indicated in **Table 3**), the estimated annual consumption values for Beijing, Rome, Las Vegas and Riyadh become 64.4 MWh, 44.1 MWh, 68.3 MWh, and 88.3 MWh, respectively.

In case of COPs, the highest values were recorded both by experiments and simulations in four consecutive months (June-September) of Riyadh, reaching experimental peak of 51.1 and simulation peak of 49 in July. The lowest COP values, on the other hand, were observed both experimentally (17.7) and by simulation (17.9) in April of Las Vegas. The COP and cooling capacity values in all the climates show an increasing trend towards warmer months of the year and decreasing trends in relatively cooler months. These trends are well justified,

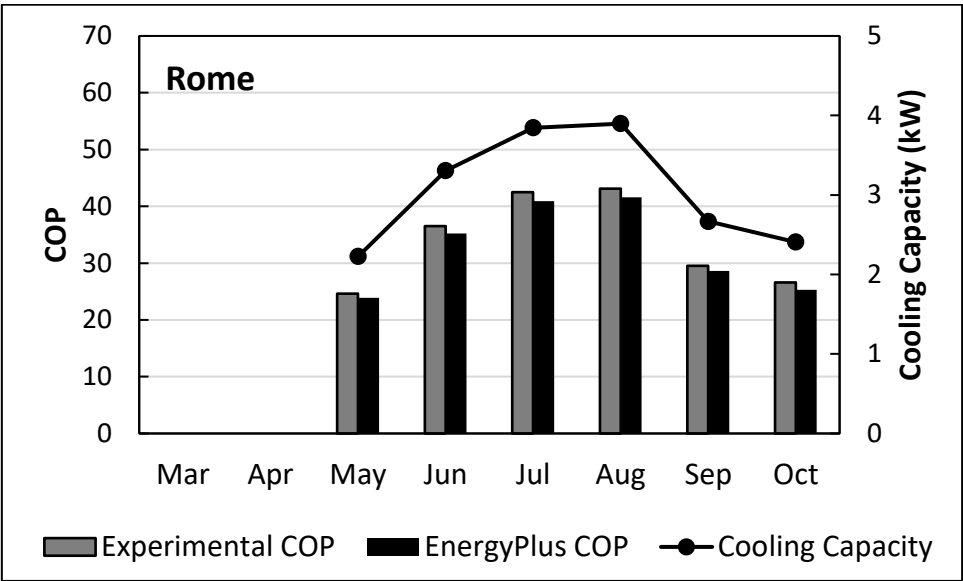
512 considering that both cooling capacity and COP are dependent on external weather  
513 conditions (**Equation 1** and **Equation 2**).



514

515

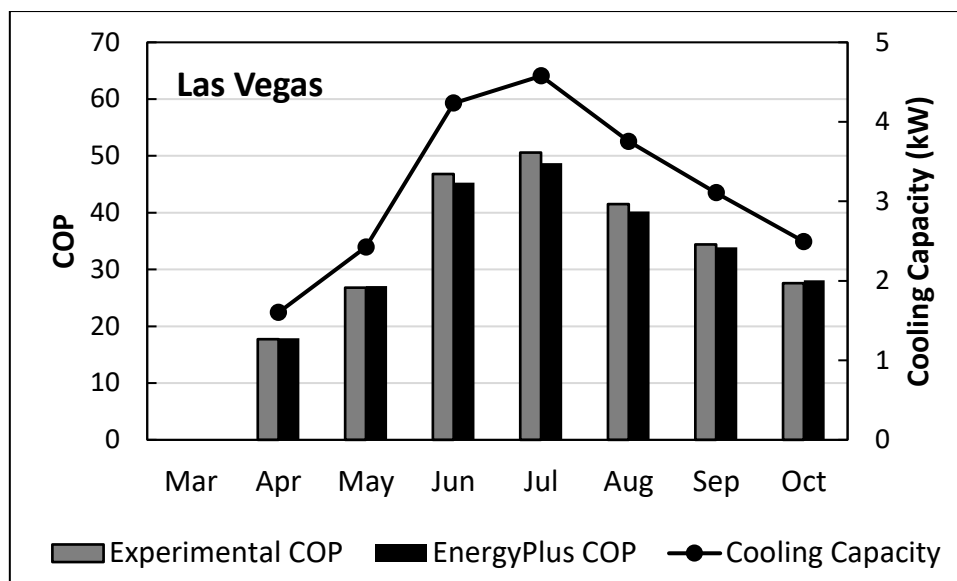
(a)



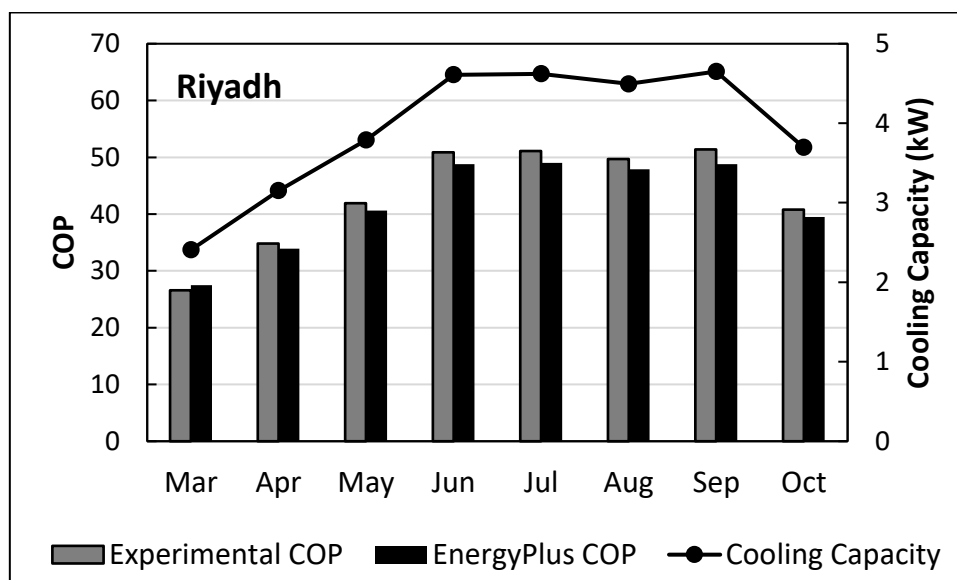
516

517

(b)



(c)



(d)

**Figure 7** Comparison of experimental COP and cooling capacity results to EnergyPlus predictions in: (a) Beijing, (b) Rome, (c) Las Vegas, and (d) Riyadh

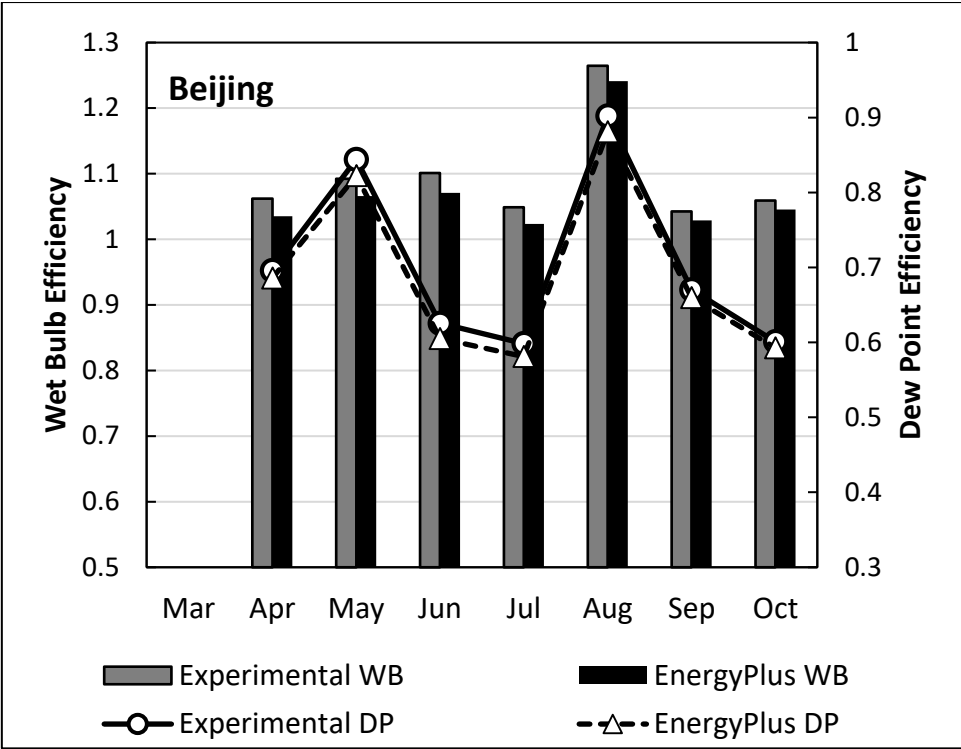
Upon careful calibration of the model, it can be seen in **Figure 7** that experimental COP results and simulation predictions are in good agreement with a maximum recorded error of 4.13% and mean error of 3.65% in Riyadh, as summarised in **Table 7**. The best fit between experiments and simulations is achieved in Beijing with mean error of 2.13% followed by Las Vegas and Rome with mean errors of 2.23% and 3.6%, respectively (**Table 7**). The simulations predict lower COP values compared to experiment results in majority of the months, except for April and May in Las Vegas and March in Riyadh where the whole



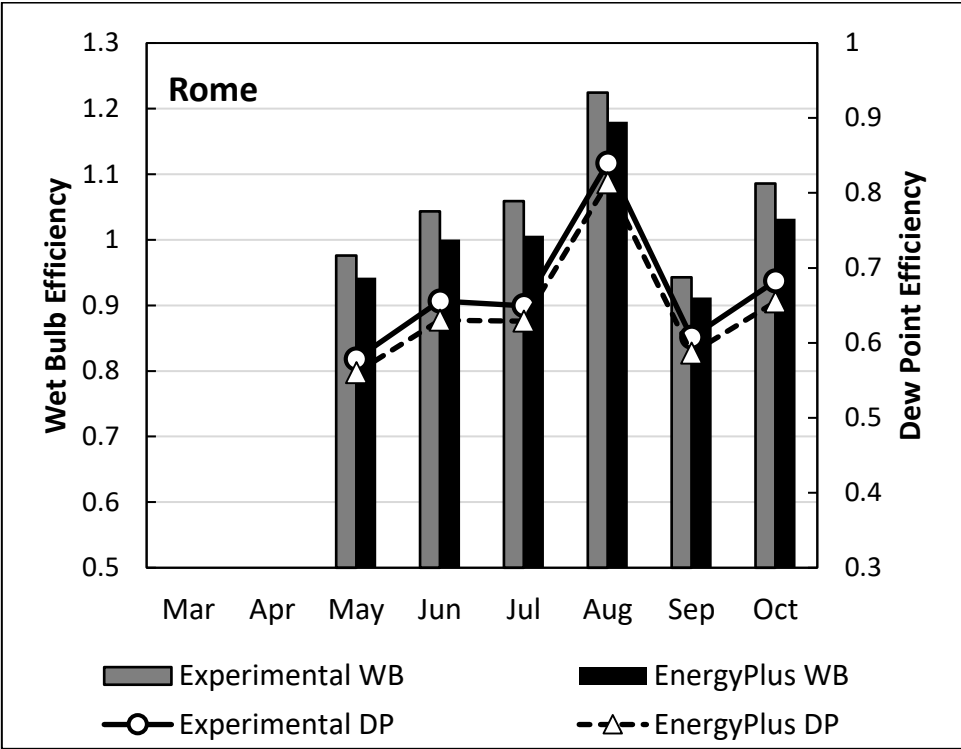
building energy model over-estimated the COP values. This can be related to the sensitivity of model to lower external temperatures and relatively low COP values in these months (<30). With higher COP values, the model tends to predict higher COP values compared to experiment results.

**Figure 8** presents the other two performance parameters of the DPC, namely the wet bulb and dew point efficiencies, which are calculated based on inlet and outlet temperatures of the system (**Equation 3** and Equation 4). As can be seen in **Figure 8**, the experimental and simulation values for both wet bulb and dew point efficiencies, in all investigated climates, are in good agreement and are following similar trends throughout the year. A look at the error values in **Table 7** reveals that, similar to COP predictions, EnergyPlus has successfully predicted the efficiencies of the system, presenting a robust case for model validation. The largest monthly difference observed between EnergyPlus and experimental results of the wet bulb and dew point efficiency are 5% (July in Rome) and 4.3% (July in Las Vegas), respectively. Overall, the whole building energy model gave the best predictions of efficiency parameters for Beijing and Las Vegas with mean error values of below 2.5%. The efficiency predictions for Las Vegas and Riyadh, despite being in validation range, showed a larger gap between experimental and simulation results with mean errors of 3.5-3.7%, as seen in **Table 7**.

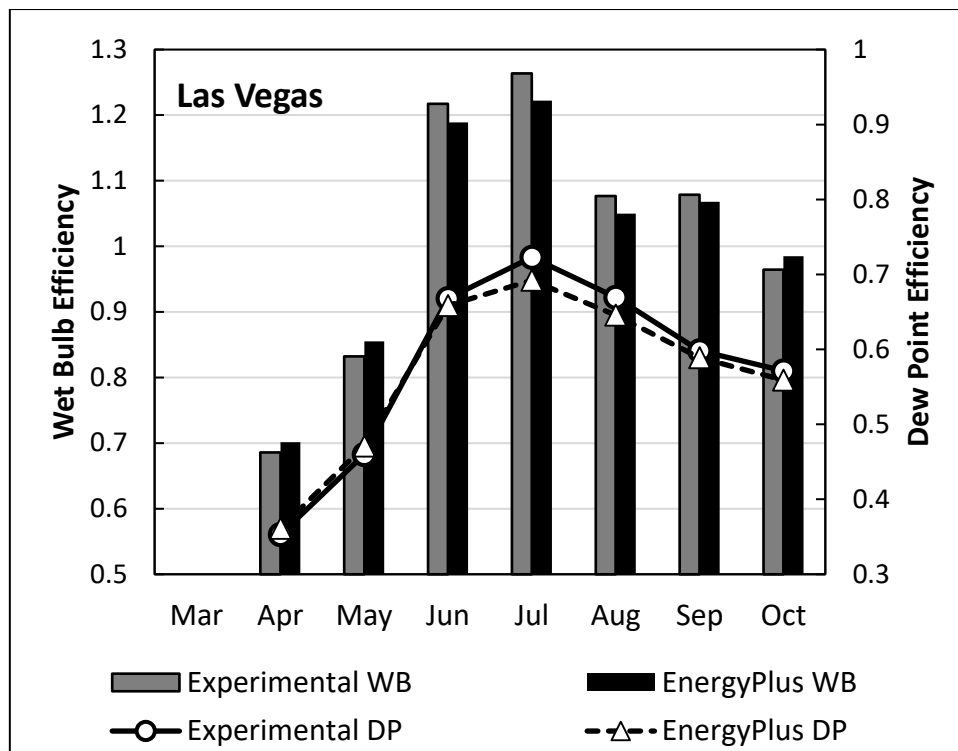
The closer investigation of the results in Figure 8, shows that both experimental and simulation results of the efficiency parameters have a steadier rate of variation in Riyadh compared to the other three climates, and hence the DPC performs at a more steady and reliable state. Such stability of operation can be related to two main factors: (i) that the mean monthly external air temperatures, which is fed to the system as working air, has less variations in Riyadh compared to the other investigated climates; and (ii) the Riyadh weather, as a hot desert climate, has the least amount of water content (i.e. humidity) compared to Beijing, Rome and Las Vegas (as seen in **Table 3**). Hence, the statement (supported by both experiments and validated whole building energy model) can be made that the dew point evaporative coolers tend to have more reliable and steady performance in hot desert climates. Such reliable and steady operation of the system, especially in high demand facilities like data centres plays a key role in effective energy management and provides flexibility in dealing with peaks of power consumption. Therefore, it can be concluded that, although higher efficiencies and COP values can be reached in some months of more moderate and humid climates, the sustained and steady operation of the investigated system is achieved in hot and dry climates.



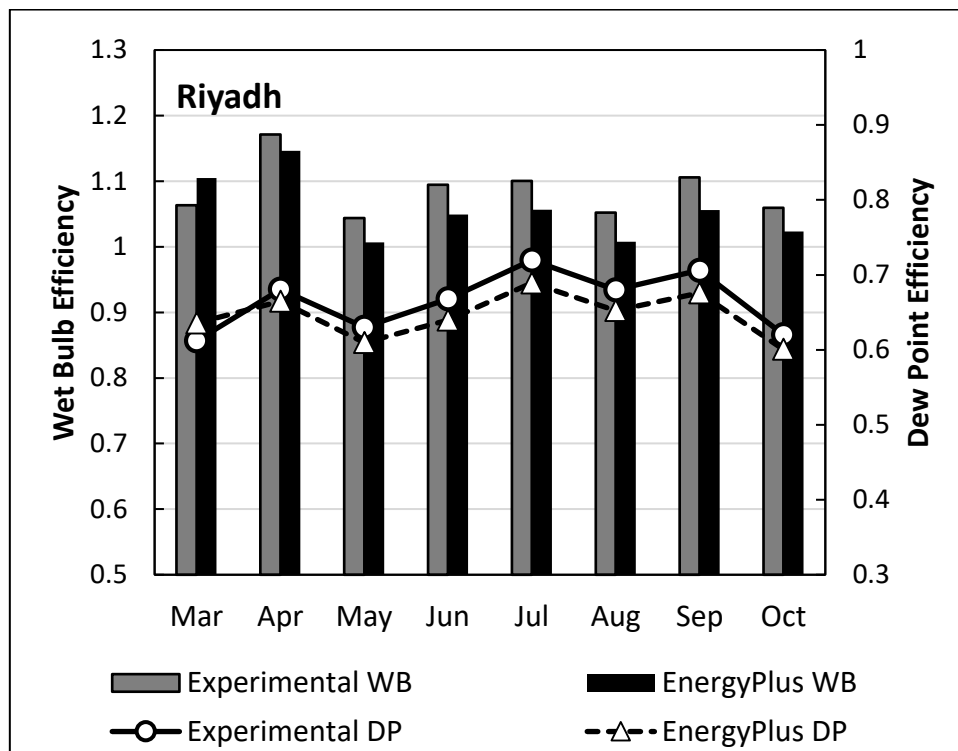
(a)



(b)



(c)



(d)

**Figure 8** Comparison of experimental wet bulb and dew point efficiencies to EnergyPlus predictions in: (a) Beijing, (b) Rome, (c) Las Vegas, and (d) Riyadh

**Table 7** Monthly and average difference between experimental values of COP, wet bulb and dew point efficiencies with EnergyPlus predictions

City	Month	COP Error (%)	Mean COP Error (%)	Wet Bulb Efficiency Error (%)	Mean Wet Bulb Efficiency Error (%)	Dew Point Efficiency Error (%)	Mean Dew- Point Efficiency Error (%)
Beijing	March	-		-		-	
	April	1.3289		2.5424		1.4799	
	May	1.4620		2.4350		2.5570	
	June	2.1053	2.1337	2.7611	2.0921	3.2614	2.2109
	July	3.9801		2.4123		2.8911	
	August	2.0290		1.8582		2.3390	
	September	1.9284		1.3427		1.5813	
	October	2.1021		1.2933		1.3643	
Rome	March	-		-		-	
	April	-		-		-	
	May	2.8455		3.4532		3.1460	
	June	3.5616	3.5984	4.1115	4.0664	3.9042	3.4793
	July	3.7647		4.9679		3.1717	
	August	3.4803		3.6269		3.1201	
	September	3.0509		3.2665		3.4744	
	October	4.8872		4.9724		4.0592	
Las Vegas	March	-		-		-	
	April	-1.1299		-2.3042		-2.3519	
	May	-1.1194		-2.7761		-2.4571	
	June	3.2051	2.2296	2.3334	2.3453	1.3627	2.5300
	July	3.7549		3.2996		4.2474	
	August	3.1325		2.5258		3.5842	
	September	1.4535		1.0105		1.5714	
	October	-1.8116		-2.1676		2.1351	
Riyadh	March	-3.3835		-3.9413		-3.8556	
	April	2.5862		2.1431		2.2921	
	May	3.1026		3.5642		3.2688	
	June	4.1257	3.6468	4.1301	3.7432	4.2079	3.6714
	July	4.1096		3.9891		4.2379	
	August	3.6217		4.2391		4.0435	
	September	5.0584		4.5035		4.3053	
	October	3.1863		3.4353		3.1603	

## *6.2. Comparison of the whole building energy model results with numerical model: superiority analysis*

In this section, the whole building energy model is compared to a previously developed numerical model of the same Dew Point Cooler (DPC) [38]. The 8<sup>th</sup> degree polynomial numerical model (described in **Section 4**) investigated the same cooling system and used the equivalent input parameters as employed by the whole building energy model. Despite the modelling work presented in this study, the numerical model lacks empirical validation and only involves an inter-model comparison to verify the results. Hence, this study offers an unprecedented opportunity to compare performance of a empirically validated whole building energy model, which takes into account the dynamic interaction of the system components with each other and also the interactions of the system with its surrounding building, to a commonly used numerical model; and provide evidence based and critical review of various modelling approaches.

The numerical model was developed based on 7857 possible operating conditions, majority of which doesn't happen in real-life operation of the system and only were considered to fully train the model [38]. The performance of the numerical model, after completing the training process was tested in the Las Vegas weather conditions, and hence here only a comparison of experiment results and models' predictions for the city of Las Vegas (Figure 9 and **Figure 10**) is presented. As can be seen in **Figure 9**, the unrestrained operating conditions employed by the numerical model can lead to COP estimates of up to two times higher than experimental values and EnergyPlus predictions. The numerical model has predicted different cooling capacities compared to the EnergyPlus and the experiments. The main reason for this lies in **Equation 1**, which shows that the cooling load is calculated based on operating parameters (various operating temperatures in this case) which has not been restricted reasonably by the numerical model. Hence, while the matching fan and pump powers are used in both models and the experiments, due to un-restricted operation parameters used by the numerical model, different cooling capacities and consequently different COPs have been predicted by the numerical model. The unrealistic COPs of 100 in June and July as estimated by the numerical model, highlights the critical need for models to take into account the restricting impact of parameters outside system operational conditions, i.e. interaction of the system with hosting building and surrounding environment. The numerical model over-estimates the COP of the system in all of the months that system was operated. The cooling capacity, however, shows a totally biased trend as it is over-estimated by the numerical model in March and April, under-estimated in May, June and July, and closely matches the experimental and EnergyPlus results in August and September (**Figure 9**).

Considering that the COP values are directly co-related to cooling capacity (**Equation 1** and **Equation 2**), it is expected that the estimates of the two performance parameters by the numerical model follow a similar trend when compared to experimental and real-life performance parameters of the system. However, the larger overall difference observed in COP estimates than the cooling capacity estimates of the numerical model when compared to experimental values suggests that the numerical model is more sensitive to cooling capacity variances when it comes to COP calculations.

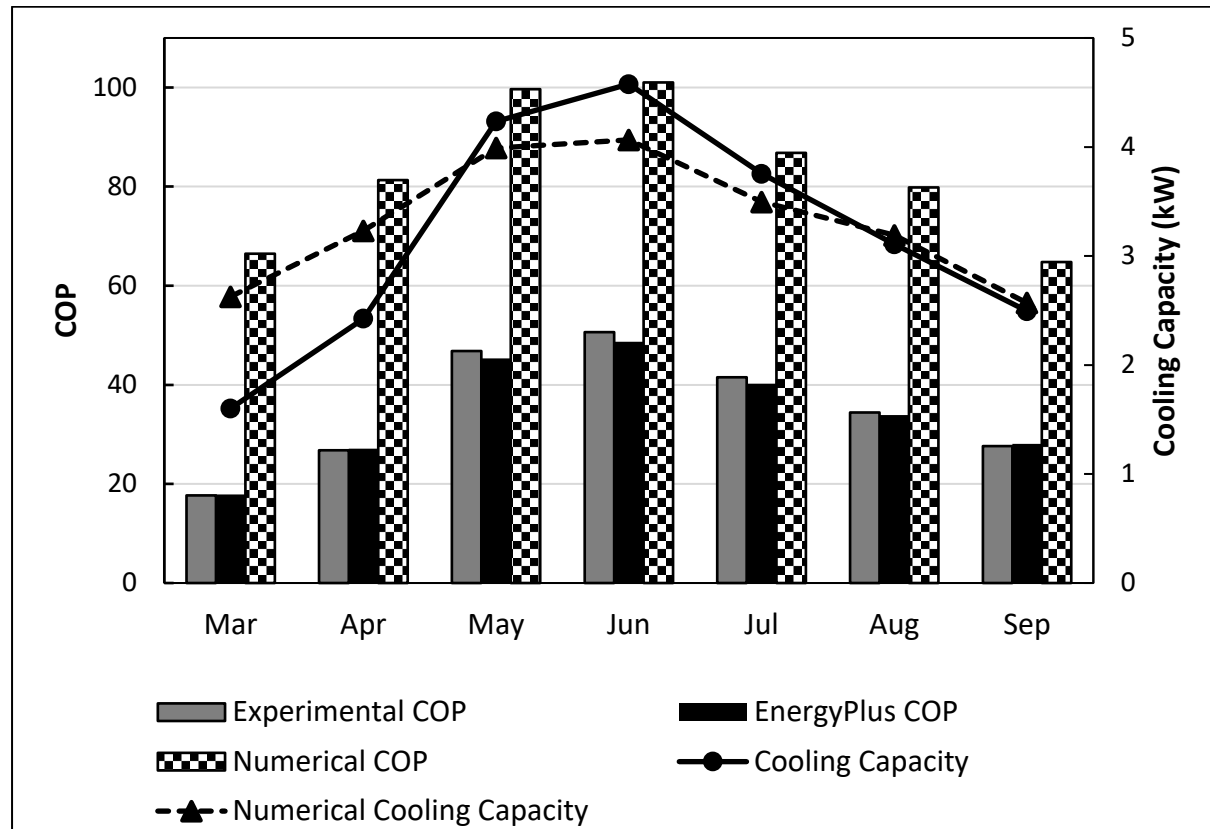


**Figure 9** Comparison of cooling capacity and COP from experiments and EnergyPlus to numerical model estimates in Las Vegas

Investigating the wet bulb and dew point efficiency estimates of the numerical model (**Figure 10**) shows that, similar to COP values, the numerical model over-estimates both efficiency values. The smallest differences between the experimental and numerical model results are recorded in May and June, and the largest difference in March and April. **Figure 10** clearly shows that while the validated EnergyPlus model predicts very close efficiencies to the experiments, the numerical model fails to produce realistic efficiency predictions in most months. The close agreement of numerical model estimates in May and June shows that the operating parameters used in these months match with the realistic values, whereas in

March and April the trained operating parameters are far from reality, resulting in poor prediction of the wet bulb and dew point efficiencies.

The randomness of the variances in numerical model errors compared to experiments and EnergyPlus results, as observed in Figure 9 and **Figure 10**, increases the confidence in concluding that the characteristics difference of the models in simulating operation of the DPC causes the recorded differences with real life operation of the system. Especially that the two models (EnergyPlus and numerical) used equivalent and matching input parameters, proves that the input parameters and unidentified uncertainties didn't have role in poor performance of the numerical model.

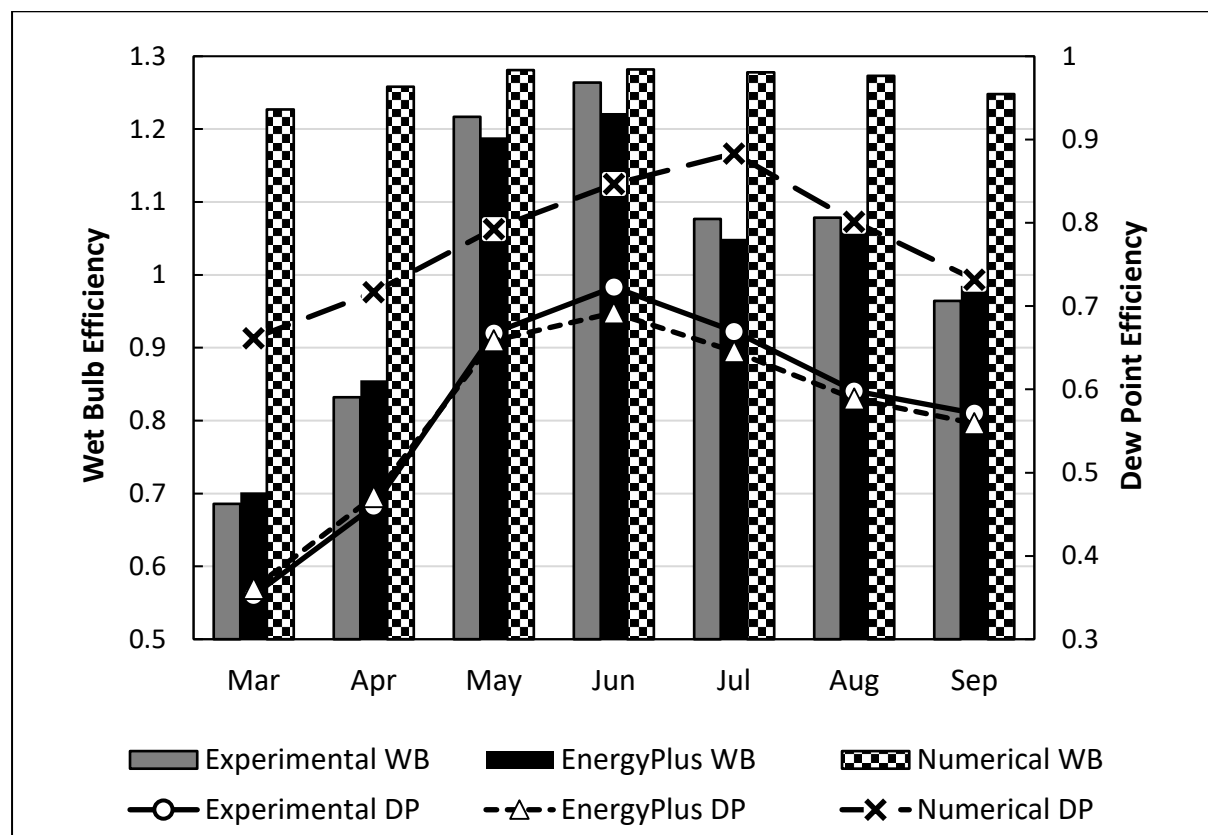


**Figure 10** Comparison of wet bulb and dew point efficiencies from experiments and EnergyPlus to numerical model estimates in Las Vegas

Having compared the whole building energy model and numerical model predictions with each other and with real-life experimental results revealed that despite numerical models' capacities in swift assessment of evaporative cooling system, these models fail to take into account the various restraining parameters which would lower the performance parameters of the investigates system. Hence, the numerical models tend to over-estimate the key performance parameters like COP, wet bulb and dew point efficiencies resulting in unrealistic and biased assessment of the system performance. The whole building energy

model developed in this study proved to better predict the performance of dew point evaporative cooler by incorporating the building-side parameters into the model and showing very close agreement with experimental performance parameters of the system.

Hence, the authors conclude with high certainty that validated whole building energy models can outperform numerical models in assessing performance of dew point evaporative coolers. These models also provide a great opportunity to investigate the system performance in a wide range of hosting buildings, from commercial buildings to schools, hospitals and office buildings, providing valuable insight into the necessary modification that might be necessary before operating the system in various buildings.

## 7. Conclusion

Faced with increasing interest in Indirect Evaporative Coolers (IECs) as a popular low energy cooling solution for high demand facilities, this study performed a modelling and experimental investigation of a state-of-the-art indirect dew point evaporative cooler. The investigated system was a high-performance counter flow Dew Point Cooler (DPC) employing a guideless and corrugated Heat and Mass Exchanger (HMX) as described in **Section 2**. The experiments were run under four different weather conditions: Beijing as humid continental climate, Rome as Mediterranean climate, Las Vegas as subtropical hot desert climate, and Riyadh as hot desert climate investigating four key performance parameters of the DPC: (i) cooling capacity, (ii) Coefficient of Performance (COP), (iii) wet bulb efficiency, and (iv) dew point efficiency (**Section 3**). The numerical model tested against the experiments was an 8<sup>th</sup> degree Multiple Polynomial Regression (MPR) model employing 6561 operational parameters as the training set and 1296 operational parameters as the validation set. The key operational parameters used in the numerical model were intake air temperature, relative humidity, and flow rate as well as Working air to intake air ratio (**Section 4**). The whole building energy model of the system and the hosting building was developed in the EnergyPlus software package which is an internationally known and tested tool for building energy simulation. The model was calibrated and validated empirically using experimental results (**Section 5**). The whole building energy model results were compared to experiments as part of model calibration and validation. The validated model was then compared to the numerical model to investigate superiority of the two approaches in predicting performance of advance dew point evaporative coolers (**Section 6**). The key findings and conclusions of the study can be summarised as:

- The highest power consumption was observed under hot desert weather conditions of the Riyadh (15.33 kW) and subtropical hot desert weather conditions of Las Vegas (13.56 kW) with cooling capacity reaching a peak of 4.6 kW in July.



- The highest COP values were recorded both by experiments and whole building energy simulations in four consecutive months (June-September) of Riyadh, reaching experimental peak of 51.1 and simulation peak of 49 in July.
- The lowest COP values were observed both experimentally (17.7) and by simulation (17.9) in April of Las Vegas.
- Experimental COP results and whole building energy simulation predictions were in good agreement with a maximum recorded error of 4.13% and mean error of 3.65% in Riyadh.
- The best COP fit between experiments and whole building energy simulations was achieved in Beijing with mean error of 2.13% followed by Las Vegas and Rome with mean errors of 2.23% and 3.6%, respectively.
- The largest difference observed between EnergyPlus and experimental results of the wet bulb and dew point efficiency are 5% (July in Rome) and 4.3% (July in Las Vegas), respectively.
- The whole building energy model gave the best predictions of efficiency parameters for Beijing and Las Vegas with mean error values of below 2.5%. The efficiency predictions for Las Vegas and Riyadh, despite being in validation range, showed a larger gap between experimental and simulation results with mean errors of 3.5-3.7%.
- The unrestrained operating conditions employed by the numerical model lead to COP estimates of up to two time higher than experimental values and EnergyPlus predictions. The numerical model over-estimates both efficiency values.
- The whole building energy model proved to better predict the performance of dew point evaporative cooler by incorporating the building-side parameters into the model.

This study proved that comprehensive validation of the numerical model (and generally any model) is a crucial part of any modelling exercise in achieving the most reliable predictions. Hence, the future work by authors will focus on developing hybrid numerical models which take into account the building side parameters and use the data from whole building energy models where necessary to develop robust numerical models capable of representing reality with high precision.

## Acknowledgments

This work was financially supported by the National Key R&D Program of China (Grant No: 2016YFE0133300); European Commission H20SCA-RISE-2016 Programme (734340-DEW-COOL-4-CDC); Department of Science and Technology of Guangdong Province, China (2018A050501002 & 2019A050509008); and UK BEIS project IEEA2021.

## References

- 722 [1] IEA, "World Energy Outlook," 2019. [Online]. Available: <https://www.iea.org/weo2019/>.  
723 [Accessed: 02-Dec-2019].
- 724 [2] L. Perez-Lombard, J. Ortiz, and C. Pout, "A review on buildings energy consumption  
725 information," *Energy Build.*, vol. 40, pp. 394–398, 2008.
- 726 [3] K. J. Chua, S. K. Chou, W. M. Yang, and J. Yan, "Achieving better energy-efficient air  
727 conditioning – A review of technologies and strategies," *Appl. Energy*, vol. 104, pp.  
728 87–104, 2013.
- 729 [4] P. Xu, X. Ma, X. Zhao, and K. Fancey, "Experimental investigation of a super  
730 performance dew point air cooler," *Appl. Energy*, vol. 203, pp. 761–777, 2017.
- 731 [5] M. I. Isaac and D. P. Van Vuuren, "Modeling global residential sector energy demand  
732 for heating and air conditioning in the context of climate change," vol. 37, pp. 507–  
733 521, 2009.
- 734 [6] M. Scott and Y. Huang, "Annex A: Technical note: methods for estimating energy  
735 consumption in buildings in effects of climate change on energy production and use in  
736 the United States. A Report by the U.S. climate change science program and the  
737 subcommittee on global change resear," Washington (DC), 2007.
- 738 [7] Y. Huang, "The impact of climate change on the energy use of the U.S. residential  
739 and commercial building sectors," Lawrence Berkeley National Laboratory, Berkeley  
740 (CA), 2006.
- 741 [8] T. Frank, "Climate change impacts on building heating and cooling energy demand in  
742 Switzerland," vol. 37, pp. 1175–1185, 2005.
- 743 [9] X. Wang, M. Zheng, W. Zhang, S. Zhang, and T. Yang, "Experimental study of a  
744 solar-assisted ground-coupled heat pump system with solar seasonal thermal storage  
745 in severe cold areas," *Energy Build.*, vol. 42, no. 11, pp. 2104–2110, 2010.
- 746 [10] L. Z. Zhang, "Energy performance of independent air dehumidification systems with  
747 energy recovery measures," vol. 31, pp. 1228–1242, 2006.
- 748 [11] K. Daou, R. Z. Wang, and Z. Z. Xia, "Desiccant cooling air conditioning : a review,"  
749 vol. 10, pp. 55–77, 2006.
- 750 [12] V. Maisotsenko, "M-CYCLE (Indirect Evaporative Cooling )," 2007. [Online]. Available:  
751 <http://www.rexresearch.com/maisotsenko/maisotsenko.htm>. [Accessed: 03-Dec-  
752 2019].
- 753 [13] E. V. Gómez, A. T. González, F. Javier, and R. Martínez, "Experimental

754 characterisation of an indirect evaporative cooling prototype in two operating modes,”  
 755 vol. 97, pp. 340–346, 2012.

756 [14] H. Campaniço, P. Hollmuller, and P. M. M. Soares, “Assessing energy savings in  
 757 cooling demand of buildings using passive cooling systems based on ventilation,” vol.  
 758 134, pp. 426–438, 2014.

759 [15] G. P. Maheshwari and R. K. Suri, “Energy-saving potential of an indirect evaporative  
 760 cooler,” vol. 69, pp. 69–76, 2001.

761 [16] L. Elberling, “Laboratory evaluation of the coolerado cooler-indirect evaporative  
 762 cooling unit,” Pacific Gas and Electric Company, 2006.

763 [17] N. J. Stoitchkov and G. I. Dimitrov, “Effectiveness of crossflow plate heat exchanger  
 764 for indirect evaporative cooling ´ des e ´ changeurs thermiques a ` plaques , a `  
 765 courants Efficacite ´ vaporatif croises pour refroidissement indirect e,” vol. 21, no. 6,  
 766 pp. 463–471, 1998.

767 [18] X. Zhao, J. M. Li, and S. B. Riffat, “Numerical study of a novel counter-flow heat and  
 768 mass exchanger for dew point evaporative cooling,” vol. 28, pp. 1942–1951, 2008.

769 [19] C. Zhan, Z. Duan, X. Zhao, S. Smith, H. Jin, and S. Riffat, “Comparative study of the  
 770 performance of the M-cycle counter- fl ow and cross- fl ow heat exchangers for  
 771 indirect evaporative cooling e Paving the path toward sustainable cooling of  
 772 buildings,” *Energy*, vol. 36, no. 12, pp. 6790–6805, 2011.

773 [20] B. Rianguilaikul and S. Kumar, “An experimental study of a novel dew point  
 774 evaporative cooling system,” *Energy Build.*, vol. 42, no. 5, pp. 637–644, 2010.

775 [21] F. Bruno, “On-site experimental testing of a novel dew point evaporative cooler,”  
 776 *Energy Build.*, vol. 43, no. 12, pp. 3475–3483, 2011.

777 [22] Y. Golizadeh, A. Badiei, X. Zhao, K. Aslansefat, X. Xiao, S. Shittu, X. Ma, “A  
 778 constraint multi-objective evolutionary optimization of a state-of-the-art dew point  
 779 cooler using digital twins” *Energy Convers. Manag.*, vol. 211, 2020.  
 780 <https://doi.org/10.1016/j.enconman.2020.112772>

781 [23] S. Moshari and G. Heidarinejad, “Numerical study of regenerative evaporative coolers  
 782 for sub-wet bulb cooling with cross- and counter- fl ow con fi guration,” *Appl. Therm.*  
 783 *Eng.*, vol. 89, pp. 669–683, 2015.

784 [24] Y. Chen, H. Yang, and Y. Luo, “Parameter sensitivity analysis and configuration  
 785 optimization of indirect evaporative cooler ( IEC ) considering condensation,” *Appl.*

786 *Energy*, vol. 194, pp. 440–453, 2017.

787 [25] A. E. Kabeel and M. Abdelgaied, “Numerical and experimental investigation of a novel  
788 configuration of indirect evaporative cooler with internal baffles,” *Energy Convers.*  
789 *Manag.*, vol. 126, pp. 526–536, 2016.

790 [26] B. Rianguilaikul and S. Kumar, “Numerical study of a novel dew point evaporative  
791 cooling system,” *Energy Build.*, vol. 42, no. 11, pp. 2241–2250, 2010.

792 [27] M. Jradi and S. Riffat, “Experimental and numerical investigation of a dew-point  
793 cooling system for thermal comfort in buildings,” *Appl. Energy*, vol. 132, pp. 524–535,  
794 2014.

795 [28] P. Xu *et al.*, “Numerical investigation of the energy performance of a guideless  
796 irregular heat and mass exchanger with corrugated heat transfer surface for dew point  
797 cooling,” *Energy*, vol. 109, pp. 803–817, 2016.

798 [29] P. Xu, X. Ma, X. Zhao, and K. S. Fancey, “Experimental investigation on performance  
799 of fabrics for indirect evaporative cooling applications,” *Build. Environ.*, vol. 110, pp.  
800 104–114, 2016.

801 [30] A. Hasan, “Going below the wet-bulb temperature by indirect evaporative cooling :  
802 Analysis using a modified e -NTU method,” *Appl. Energy*, vol. 89, no. 1, pp. 237–245,  
803 2012.

804 [31] J. Lin, K. Thu, T. D. Bui, R. Z. Wang, K. C. Ng, and K. J. Chua, “Study on dew point  
805 evaporative cooling system with counter-flow configuration,” vol. 109, pp. 153–165,  
806 2016.

807 [32] X. Cui, K. J. Chua, and W. M. Yang, “Numerical simulation of a novel energy-efficient  
808 dew-point evaporative air cooler,” *Appl. Energy*, vol. 136, pp. 979–988, 2014.

809 [33] J. Lin *et al.*, “Unsteady-state analysis of a counter- fl ow dew point evaporative cooling  
810 system,” vol. 113, pp. 172–185, 2016.

811 [34] D. Pandelidis and S. Anisimov, “Numerical analysis of the heat and mass transfer  
812 processes in selected M-Cycle heat exchangers for the dew point evaporative  
813 cooling,” *Energy Convers. Manag.*, vol. 90, pp. 62–83, 2015.

814 [35] D. Pandelidis and S. Anisimov, “Numerical study and optimization of the cross-flow  
815 Maisotsenko cycle indirect evaporative air cooler,” *Int. J. Heat Mass Transf.*, vol. 103,  
816 pp. 1029–1041, 2016.

817 [36] A. Sohani, H. Sayyaadi, and S. Hoseinpoori, “Modeling and multi-objective

818 optimization of an M-cycle cross-flow indirect evaporative cooler using the GMDH  
819 type neural network Modélisation et optimisation à objectifs multiples d ' un  
820 refroidisseur évaporatif indirect à écoulements croisés à cycle M en utilisant le réseau  
821 neuronal de type GMDH," *Int. J. Refrig.*, vol. 69, pp. 186–204, 2016.

822 [37] X. Cui, K. J. Chua, W. M. Yang, K. C. Ng, K. Thu, and V. T. Nguyen, "Studying the  
823 performance of an improved dew-point evaporative design for cooling application,"  
824 vol. 63, pp. 624–633, 2014.

825 [38] Y. Golizadeh, X. Ma, X. Zhao, and S. Shittu, "A statistical model for dew point air  
826 cooler based on the multiple polynomial regression approach," *Energy*, vol. 181, pp.  
827 868–881, 2019.

828 [39] Y. Golizadeh, X. Zhao, S. Shittu, A. Badiei, M. E. G. V Cattaneo, and X. Ma,  
829 "Statistical investigation of a dehumidification system performance using Gaussian  
830 process regression," *Energy Build.*, vol. 202, p. 109406, 2019.

831 [40] ASHRAE, "American Society of Heating Refrigerating and Air-Conditioning Engineers:  
832 Handbook of Fundamentals, SI edition," Atlanta, GA, USA, 2009.

833 [41] ASHRAE, "American Society of Heating Refrigerating and Air-Conditioning Engineers:  
834 TC9.9 Data Center Power Equipment Thermal Guidelines and Best Practices,"  
835 Atlanta, GA, USA, 2016.

836 [42] A. Pakari and S. Ghani, "Regression models for performance prediction of counter fl  
837 ow dew point evaporative cooling systems," *Energy Convers. Manag.*, vol. 185, no.  
838 November 2018, pp. 562–573, 2019.

839 [43] K. P. Moustris, P. T. Nastos, I. K. Larissi, and A. G. Paliatsos, "Application of Multiple  
840 Linear Regression Models and Artificial Neural Networks on the Surface Ozone  
841 Forecast in the Greater Athens Area , Greece," vol. 2012, 2012.

842 [44] NREL, "EnergyPlus Version 9.0.1," 2018. [Online]. Available:  
843 <https://github.com/NREL/EnergyPlus/releases/tag/v9.0.1>. [Accessed: 07-Jan-2020].

844 [45] DesignBuilder, "DesignBuilder user manual Version 6. UK: DesignBuilder software  
845 limited." [Online]. Available: <https://designbuilder.co.uk/helpv6.0/>. [Accessed: 07-Jan-  
846 2020].

847 [46] EnergyPlus, "Auxiliary EnergyPlus Programs." [Online]. Available:  
848 [https://energyplus.net/sites/default/files/pdfs\\_v8.3.0/AuxiliaryPrograms.pdf](https://energyplus.net/sites/default/files/pdfs_v8.3.0/AuxiliaryPrograms.pdf).  
849 [Accessed: 07-Jan-2020].

- 850 [47] BSI, "BS EN 12831: Heating systems in buildings — Method for calculation of the  
851 design heat load. The British Standards Institution.," 2013.
- 852 [48] ASHRAE, "International weather for energy calculations. American Society of Heating,  
853 Refrigerating and Air-Conditioning Engineers, Atlanta, GA, ASHRAE," 2001. [Online].  
854 Available: [https://www.ashrae.org/technical-resources/bookstore/ashrae-international-](https://www.ashrae.org/technical-resources/bookstore/ashrae-international-weather-files-for-energy-calculations-2-0-iwec2)  
855 [weather-files-for-energy-calculations-2-0-iwec2](https://www.ashrae.org/technical-resources/bookstore/ashrae-international-weather-files-for-energy-calculations-2-0-iwec2). [Accessed: 09-Jan-2020].
- 856 [49] A. Badiei, D. Allinson, and K. J. Lomas, "Automated dynamic thermal simulation of  
857 houses and housing stocks using readily available reduced data," *Energy & Buildings*  
858 vol. 203, 2019. <https://doi.org/10.1016/j.enbuild.2019.109431>
- 859 [50] BRE, "The Government's Standard Assessment Procedure for Energy Rating of  
860 Dwellings (SAP 2012). Garston, Watford, WD25 9XX, UK.," 2012. [Online]. Available:  
861 [https://www.bre.co.uk/filelibrary/SAP/2012/SAP-2012\\_9-92.pdf](https://www.bre.co.uk/filelibrary/SAP/2012/SAP-2012_9-92.pdf). [Accessed: 10-Jan-  
862 2020].